Biomechanics and Modeling in Mechanobiology
https://doi.org/10.1007/s10237-022-01638-6

ORIGINAL PAPER

Approximating subject-specific brain injury models via scaling based on head–brain morphological relationships

Shaoju Wu[1] · Wei Zhao[1] · Zheyang Wu[2] · Thomas McAllister[3] · Jingwen Hu[4,5] · Songbai Ji[1,6]

Received: 25 March 2022 / Accepted: 7 September 2022

Abstract

Most human head/brain models represent a generic adult male head/brain. They may suffer in accuracy when investigating traumatic brain injury (TBI) on a subject-specific basis. Subject-specific models can be developed from neuroimages; however, neuroimages are not typically available in practice. In this study, we establish simple and elegant regression models between brain outer surface morphology and head dimensions measured from neuroimages along with age and sex information ($N = 191$; 141 males and 50 females with age ranging 14–25 years). The regression models are then used to approximate subject-specific brain models by scaling a generic counterpart, without using neuroimages. Model geometrical accuracy is assessed using adjusted R^2 and absolute percentage error (e.g., 0.720 and $3.09 \pm 2.38\%$, respectively, for brain volume when incorporating tragion-to-top). For a subset of 11 subjects (from smallest to largest in brain volume), impact-induced brain strains are compared with those from "morphed models" derived from neuroimage-based mesh warping. We find that regional peak strains from the scaled subject-specific models are comparable to those of the morphed counterparts but could be considerably different from those of the generic model (e.g., linear regression slope of 1.01–1.03 for gray and white matter regions versus 1.16–1.19, or up to ~ 20% overestimation for the smallest brain studied). These results highlight the importance of incorporating brain morphological variations in impact simulation and demonstrate the feasibility of approximating subject-specific brain models without neuroimages using age, sex, and easily measurable head dimensions. The scaled models may improve subject specificity for future TBI investigations.

Keywords Concussion · Brain injury model · Subject-specific model · Head morphology · Worcester head injury model (WHIM)

1 Introduction

Sixty-nine million people worldwide are estimated to suffer traumatic brain injury (TBI) each year (Dewan et al. 2019), with ~ 75% of them mild TBI (mTBI) (Laker 2011). In the USA alone, more than 200 million adults and children participate in organized physical activities (Centers for Disease Control and Prevention 2007). Sports and recreation activities are major causes of mTBI, which is often referred to as concussion. There are nearly 4 million concussion incidents annually (Langlois et al. 2006), which is likely underestimated because of the significant under-reporting issue (Ferdinand Pennock et al. 2020). Studies have also suggest that females are, in general, at a greater risk of concussion than males (Iverson et al. 2017).

There is general consensus that impact-induced "brain strain" is the primary cause of brain injury, including mTBI (Ji et al. 2022). A viable approach to estimating

✉ Songbai Ji
sji@wpi.edu

1 Department of Biomedical Engineering, Worcester Polytechnic Institute, 60 Prescott Street, Worcester, MA 01609, USA

2 Mathematical Sciences, Worcester Polytechnic Institute, Worcester, MA 01609, USA

3 Department of Psychiatry, Indiana University School of Medicine, Indianapolis, IN 46202, USA

4 University of Michigan Transportation Research Institute, Ann Arbor, MI 48109, USA

5 Department of Mechanical Engineering, University of Michigan, Ann Arbor, MI 48109, USA

6 Department of Mechanical Engineering, Worcester Polytechnic Institute, Worcester, MA 01609, USA

Published online: 06 October 2022

injury-causing brain strains in live humans is through impact simulation using a validated brain model. Over the past half-century, numerous finite element (FE) brain models have been developed (Yang et al. 2006; Ji et al. 2022). Model sophistications have also steadily increased, with recent advancements to incorporate more anatomical details such as sulci (Miller et al. 2016; Ghajari et al. 2017; Li et al. 2020), cerebral vasculatures (Zhao and Ji 2022), white matter material property anisotropy (Giordano et al. 2017; Zhao and Ji 2019), more realistic brain-skull boundary conditions (Zhou et al. 2019), explicit modeling of white matter fibers (Wu et al. 2019b; Garimella et al. 2019), mesh conformity of internal anatomical boundaries (Atsumi et al. 2018; Li et al. 2020), among others.

Nevertheless, most models represent a generic, 50th-percentile male head (Ji et al. 2022) and they do not account for variance in brain morphology. Therefore, these models may suffer in accuracy when investigating injury risks on a subject-specific basis, especially for youth (Rowson and Duma 2020) and females (Mollayeva et al. 2018) due to the anticipated larger morphological differences relative to the generic adult male head (Rollins et al. 2010) and the significance of model geometry on brain responses. For example, brain size is linearly related to pressure from linear acceleration (Bradshaw and Morfey 2001; Zhao et al. 2015). Increasing brain size significantly increases maximum effective stress (Kleiven and von Holst 2002) and strain (Li et al. 2020; Liu et al. 2021, 2022). Significant variations also exist in the spatiotemporal locations of peak strains due to disparities in brain shape (Li et al. 2020). Collectively, these findings highlight the importance of accounting for strain differences resulting from head and brain morphological variations.

To do so, a generic model can be scaled linearly (Kleiven and von Holst 2002) or following affine (Danelson et al. 2008) or nonrigid registration through mesh warping (Li et al. 2011, 2016, 2020; Ji et al. 2015; Alshareef et al. 2021; Li 2021; Liu et al. 2022). Subject-specific models can also be developed directly from individual neuroimages using a conventional meshing process (Ji et al. 2011; Li et al. 2020) or converting voxels directly into hexahedral elements (Miller et al. 2016) with additional surface voxel smoothing to mitigate numerical artifacts (Chen and Ostoja-Starzewski 2010). Linear scaling does not require neuroimages, which is also commonly applied when validating a model against experimental data (Zhao and Ji 2020; Alshareef et al. 2021) when no neuroimages are publicly available (Hardy et al. 2007; Knutsen et al. 2014; Chan et al. 2018; Alshareef et al. 2018). For simple scaling, basic information about head or brain morphology such as length and width would suffice. Neuroimage-based methods are expected to improve model geometrical accuracy. Nevertheless, they require individual neuroimages that may not always be available. This could pose challenges for practical use.

When information on head and brain dimensions does not exist or no neuroimages are available, an alternative strategy to estimate head and brain size is through a pre-established statistical model. For example, age-based regression models (Danelson et al. 2008) were developed from manual measurements in a series of axial MRI for both males and females. They enabled deriving shape- and size-related scaling factors for multiple brain regions. This allowed scaling the SIMon adult head model (Takhounts et al. 2008) to match with pediatric brains in multiple age groups from newborns to 21 years old. However, model geometrical accuracy may suffer because the statistical models do not account for individual variations beyond age and sex (Rollins et al. 2010). A recent work systematically analyzed scalp and skull inner surfaces of 101 adolescents and young adults (14–25 years old) segmented from CT (Liu et al. 2022). The study identified that the size of the head and brain, tragion-to-top distance, as well as head length and breadth are the top principal components most significantly influencing head geometric variations. Consistent with other studies, brain size was found to significantly correlate with peak maximum principal strain (MPS) of the whole brain.

Therefore, these investigations motivate our current study to further develop statistical models between measurements of brain outer surface morphological features and those of the head, beyond age and sex alone. The additional head dimensions are expected to improve accuracy over those using information only about age and sex (Danelson et al. 2008). An important advantage of the approach is that, once the statistical models are established, subject-specific models can be approximated by scaling a generic model to match with an individual brain, and without relying on neuroimages. This could make the technique valuable to improve subject specificity when no neuroimages are available in practice. To assess accuracy, 11 subjects were selected to create subject-specific models by scaling (based on external head dimensions along with age and sex, or age and sex only as a comparison (Danelson et al. 2008)). They were compared with the generic model as well as the corresponding baseline subject-specific models developed from the more sophisticated mesh warping method (Ji et al. 2015). A concussive head impact is used for impact simulation, based on which to quantify the accuracy improvement. This study contributes toward improving subject specificity for brain models in future TBI investigations.

2 Methods

The overall procedure of this study is illustrated in Fig. 1. First, the head and brain morphologies were measured semi-automatically based on individual high-resolution

neuroimages. These measures, along with subject's age and sex information, were used to establish statistical models via stepwise regression. The quality of the regression models was assessed by comparing predicted brain geometric measures with the actual measurements. A subset of subjects were then selected to approximate subject-specific models via simple scaling based on the baseline anisotropic Worcester head injury model (WHIM) V1.0 (Zhao and Ji 2019), and without neuroimages. Their accuracy in terms of impact-induced brain strains was compared with those from corresponding morphed subject-specific models created from image-based mesh warping, as well as with those from the generic model. The details of each step are described in subsections below (Fig. 1).

2.1 Worcester head injury model (WHIM)

The anisotropic WHIM Version 1.0 (Zhao and Ji 2019) was used as the baseline generic model. It uses the same mesh from the isotropic counterpart (Ji et al. 2015), which was created with high mesh quality and geometrical accuracy based on high-resolution T1-weighted magnetic resonance image (MRI) of a concussed athlete. The details of mesh quality in terms of element warpage, aspect ratio, skew, minimum length, Jacobian, and minimum and maximum angles have been reported previously (Ji et al. 2015). In total, the brain contains 56.6 k nodes and 55.1 k hexahedral elements with an average element size of 3.3 ± 0.79 mm (Fig. 1). The WHIM was recently validated against a wide-range of blunt impact conditions, including relative brain-skull displacement and marker-based strain in high- and mid-rate cadaveric impacts, as well as strain from in vivo head rotations (Zhao and Ji 2020). It achieves an average peak strain magnitude ratio (simulation vs. experiment) of 0.94 ± 0.30 based on marker-based strains in 12 cadaveric impacts. A ratio of 1.00 ± 0.00 would indicate an identical peak response relative to experiment (albeit errors in experimental data, themselves, should not be ignored). The head coordinate system

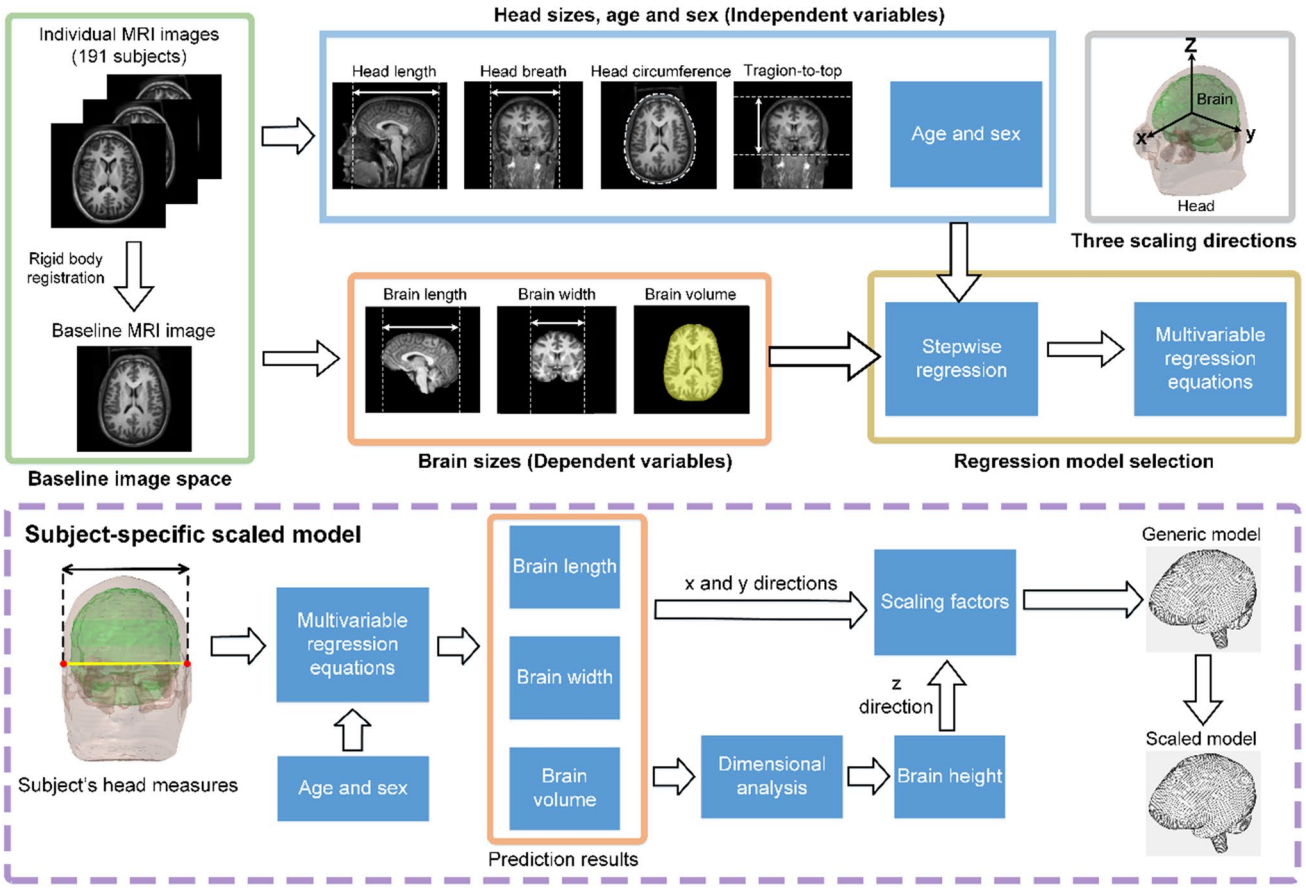

Fig. 1 Overview of the semi-automatic head and brain morphological measurements and regression-based scaling to approximate subject-specific models via linear scaling along the three anatomical directions. The baseline MRI is used as a template for rigid registration to facilitate consistent measurement of head and brain dimensions and does not directly contribute to the multivariable regression models. Instead, the brain dimensions of the generic model from the baseline MRI serve as reference to derive scaling factors. The resulting scaled model approximates subject-specific brain model for the individual

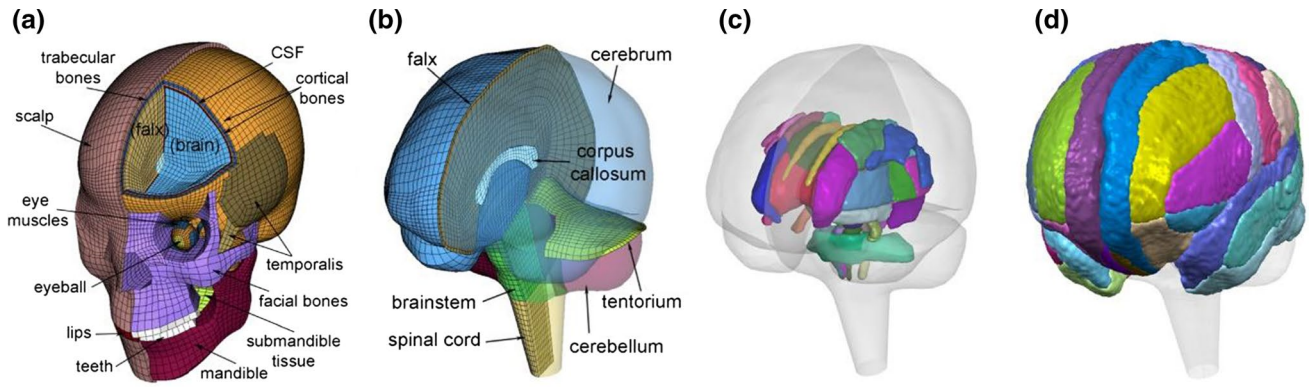

Fig. 2 The Worcester Head Injury Model (WHIM) showing the head exterior (**a**), intracranial components (**b**), 50 deep white matter regions (**c**), and (**d**) 54 cortical gray matter regions

was chosen such that the posterior-to-anterior, right-to-left, and inferior-to-superior directions corresponded to the x, y, and z directions, respectively. Deep white matter (WM) and cortical gray matter (GM) regions have been previously identified by co-registering with the corresponding neuroimage atlases (Zhao et al. 2017; Wu et al. 2020).

2.2 Head and brain morphological measurements

Neuroimage acquisitions were part of the previous effort to investigate the biomechanical basis of mild TBI in collegiate and high school contact sport athletes. Data from varsity athletes on the Dartmouth College football team and men's and women's ice hockey teams, and the Hanover High School football team were collected between 2007 and 2011 as reported previously (McAllister et al. 2012). T1-weighted MR images (isotropic resolution of 1.5 mm × 1.5 mm × 1.5 mm, with image dimension of 112 × 171 × 171) were collected from 191 subjects (141 males, 14–25 years old; 50 females, 18–24 years old; approved by the Institutional Review Board at Dartmouth College).

2.3 Head and brain morphological measurements

To facilitate consistent measurement, the T1-weighted MRI used to develop the WHIM (Ji et al. 2015) was first rigidly rotated so that the Frankfort plane was horizontal. Using the rotated MRI as a template, individual MRI images of each subject were then rigidly registered in FSL. This rigid registration did not alter any head or brain morphology but ensured a consistent head orientation to facilitate subsequent semi-automatic measurements.

For a given subject, head and brain morphological features including head breadth (left-to-right), length (anterior-to-posterior) and circumference as well as brain width, length and volume were measured following the same procedures detailed in previous studies (Rivara et al. 1999; Tang et al. 2010; Thai et al. 2015). Briefly, an axial plane having the largest head circumference was first selected (Fig. 3) based on which to measure: (1) the head breath as the maximum distance between the left and right temples above the ear; (2) the head and brain lengths as the maximum distance in the anterior–posterior direction; (3) the brain width as the horizontal distance between the left and right poles on the axial plane; and (4) the head circumference measured as the boundary length of the head on the selected axial plane. Finally, the brain volume was also determined from the BET (Brain Extraction Tool) segmentation by first removing non-brain tissues (Smith 2002). Intuitively, providing additional information of the head dimension in the inferior-superior direction would improve the quality of statistical models (Liu et al. 2022). Therefore, tragion-to-top distance was also measured as illustrated in Fig. 3 (Lee et al. 2006). Figure 4 summarizes the histograms of subjects across the age range for male and female subjects, as well as the various head and brain morphological measurements across the value ranges.

2.4 Multivariate linear regression models

Stepwise regression (Draper and Smith 1998) was used to establish statistical models between the measured brain dimensions and those of the head, along with age and sex. The technique begins with a single independent variable and then iteratively adds or removes another independent variable to select the best subset to construct multivariable linear regression equations according to the Bayesian information criterion (BIC) (Draper and Smith 1998). This criterion heavy penalizes complex regression models to minimize model overfitting.

Tragion-to-top distance is a significant principal component in skull geometrical variation (Liu et al. 2022). Nevertheless, this feature may not be typically measured on the sports field (Collins et al. 2014). Therefore, we fitted two separate sets of regression models by either including or

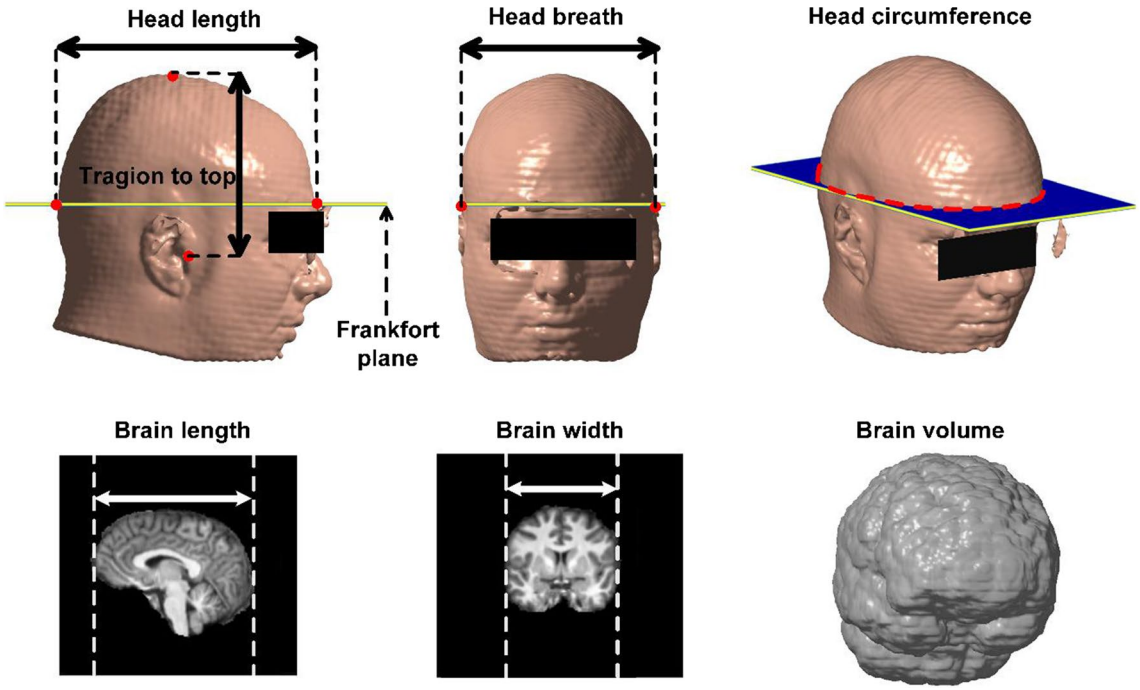

Fig. 3 Illustration of various measurements of the head (top) and brain (bottom) based on surface rendering of the scalp from T1-weighted MRI as well as mid-sagittal and coronal images. An axial plane of the largest head circumference was used determine the head/brain length, head breath, brain width, and head circumference. Tragion-to-top was measured as the distance between the tragion and the top of the head. Brain volume was measured based on the segmented brain

excluding tragion-to-top distance. As a comparison, a third set of regression models was also generated to only consider age and sex (Danelson et al. 2008). Adjusted coefficient of determination (adjusted R^2) was used to evaluate the regression performance. In addition, absolute percentage error (APE) between predicted and measured brain dimension was also reported.

2.5 Approximating subject-specific models by linear scaling

Eleven subjects with brain volume ranging from the smallest to the largest ($N=11$; 7 males and 4 females) were selected to generate subject-specific brain models. Their descriptive statistics are reported in Table 1. Statistics for the "generic subject" used to develop the baseline WHIM are also shown, which are close to the average values of the 11 subjects, as expected.

Linear scaling factors along the three orthogonal directions, x, y, and z were used to scale the generic WHIM (Fig. 1). First, the scaling factors along the x and y directions for brain length (α_1) and width (α_2), respectively, were readily available from the established regression models. They were determined by the ratio of the predicted brain length and width with respect to their counterparts from the generic subject.

$$\alpha_1 = \frac{l_b}{L_b} \text{ and } \alpha_2 = \frac{w_b}{W_b} \tag{1}$$

where L_b and W_b are the length and width of the brain derived from the baseline MRI; l_b and w_b are the predicted length and width of the brain from the regression models of a given individual subject.

To obtain the scaling factor along the z direction, α_3, a dimensional analysis was used. Brain volume is expected to be proportional to the product of brain length, width, and the third dimension referred to as "brain height." This is given as below:

$$\frac{v_b}{V_b} = \frac{l_b}{L_b} \times \frac{w_b}{W_b} \times \frac{h_b}{H_b} \tag{2}$$

where V_b and v_b are the brain volume derived from the generic subject and that predicted from the regression model, respectively; H_b and h_b are the "brain height" from the baseline and subject-specific MRI, respectively. Their actual values are not necessary to derive their ratio, α_3, which can be approximated via the dimensional analysis according to the following equation:

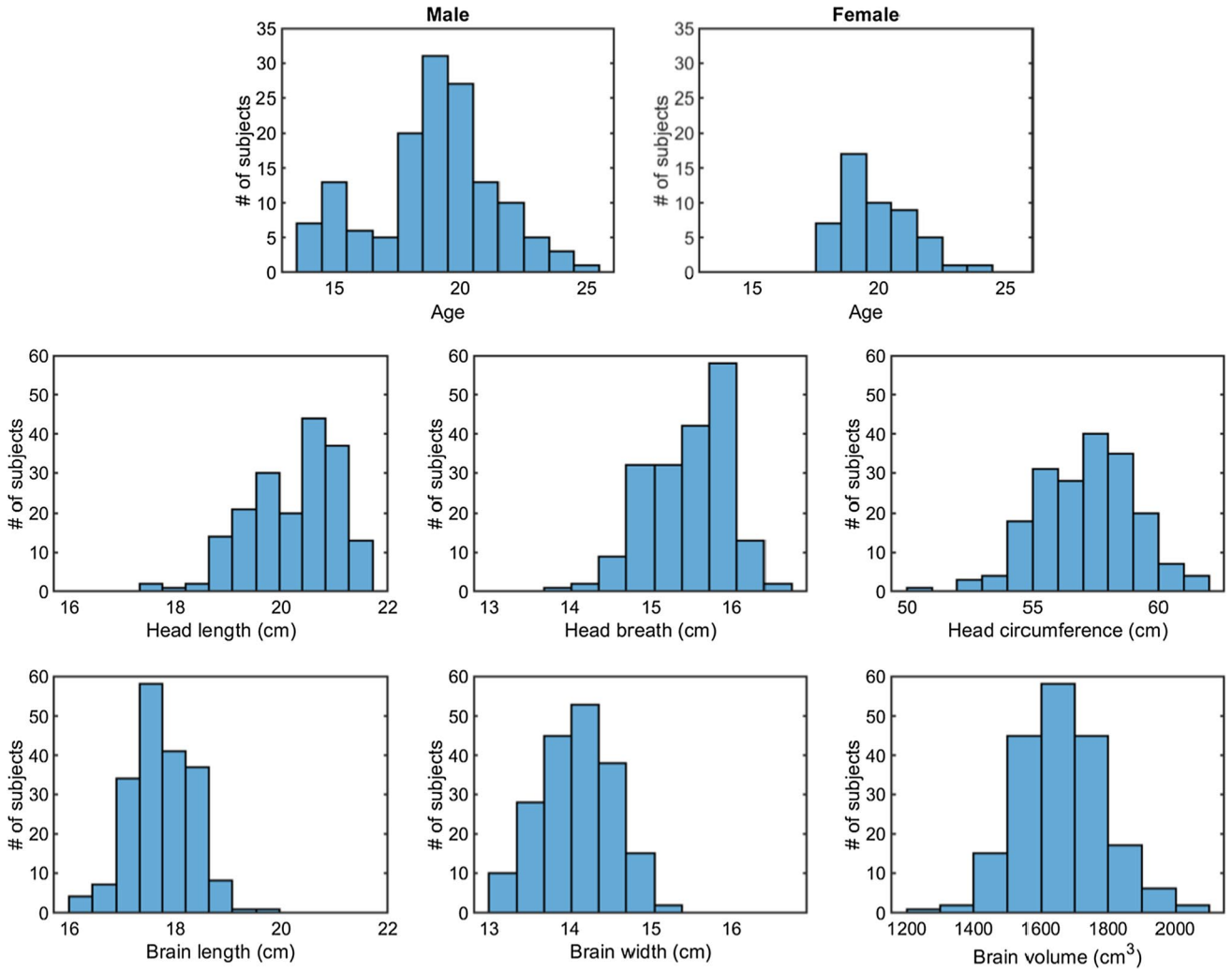

Fig. 4 Histograms of the number of male ($N=141$) and female ($N=50$) subjects across the age range (top) and various head (middle) and brain (bottom) morphological measurements across the value ranges

Table 1 Summary of the various head and brain measurements (units are in cm or cm^3 for volume) and age (in years) for the 11 selected subjects (7 males and 4 females) with the brain volume ranging from the smallest to the largest. Statistics of the "generic subject" used to develop the baseline WHIM are also reported (in parenthesis)

	Head length	Head breadth	Head circumference	Tragion-to-top
Range	17.7–21.6	13.8–16.2	50.6–61.2	11.7–15.2
mean ± std	20.1 ± 1.1	15.4 ± 0.8	57.0 ± 3.0	13.6 ± 0.6
(Generic)	(19.8)	(15.0)	(55.66)	(12.3)
	Brain length	Brain width	Brain volume	Age
Range	16.1–18.6	13.1–15.0	1223.2–2049.9	14–25
mean ± std	17.6 ± 0.7	14.1 ± 0.6	1662.9 ± 88.1	19.3 ± 2.9
(Generic)	(17.7)	(13.7)	(1618.1)	(18)

$$\alpha_3 = \frac{h_b}{H_b} = \frac{v_b/V_b}{w_b/W_b \times l_b/L_b} \tag{3}$$

Three sets of scaling factors were obtained from the three sets of statistical regression models: (1) with or (2) without tragion-to-top distance measures as model feature input, and (3) using only age and sex in the regression models.

2.6 Baseline subject-specific models by mesh warping

In addition, subject-specific models via mesh warping (Ji et al. 2015) were also generated ("morphed models") for the selected 11 subjects. An affine registration and an additional B-spline nonrigid registration were executed to generate the deformation field, which was then used to warp the mesh nodes of the generic model (Ji et al. 2015). The morphed models were considered as more geometrically "accurate" and were used as baselines to assess the impact simulation accuracy.

2.7 Comparison among scaled and morphed subject-specific models and the generic model

The scaled models and their morphed counterparts were compared in terms of impact-induced brain strains. A representative concussive head impact from the reanalyzed National Football League (NFL) dataset (Sanchez et al. 2018) was used for simulation. This impact was a predominantly sagittal concussive impact, with peak linear acceleration, rotational acceleration and rotational velocity of 1041.7 m/s^2, 5860.9 rad/s^2, and 42.3 rad/s, respectively. The impact kinematic profiles are reported in the Supplementary (Fig. S1). First, peak MPS values of the whole brain from the two sets of models were compared, as this strain measure currently serves as the de facto benchmark to assess the quality of numerous kinematics-based injury metrics (Bian and Mao 2020; Fahlstedt et al. 2021). Accuracy was assessed using coefficients of determination (R^2) and root mean squared error (RMSE).

To further examine differences in regional peak strains, peak MPS in the 50 deep white matter (WM) regions of interests (ROIs) and 54 Gy matter (GM) ROIs were also compared. These anatomical regions were identified based on the generic WHIM using the co-registered ICBM WM (Varentsova et al. 2014) and LPBA40 GM atlases (Shattuck et al. 2008), respectively. The details of the image registration and identification of the anatomical regions were reported previously (Zhao et al. 2017; Wu et al. 2020). Mesh elements corresponding to each ROI remained identical in the scaled, morphed, and generic models. Linear regressions were performed between MPS values in the WM and GM ROIs. In addition to R^2 and RMSE, the regression slope (k) was also reported to indicate an overall under- or overestimation relative to the baseline. For all comparisons, the generic model was also used as a reference.

2.8 Data analysis

The qualities of the three regression models for predicting individual brain length, width, and volume were compared using adjusted R^2 and mean absolute percentage errors (MAPE) relative to the actual measurements for the entire dataset. For each prediction method, the number of subjects that exceeded 5% and 10% MAPE was also reported to highlight their performance differences. The generic model was used as a reference for comparison.

For the selected 11 subjects, whole-brain and regional peak MPS (assessed at the 95th-percentile level) from the scaled models were compared with those from the morphed models as well as the generic WHIM. Since we expected scaled models to improve performance, one-tailed t-test with Bonferroni correction was used for performance comparisons among different regression models. F-test of equality of variances was also conducted when needed. In all statistical tests, significance was defined at the family-wise level of 0.05. All impact simulations were conducted in Abaqus (Version 2018; Dassault Systèmes, France), and all data analyses were performed in MATLAB (R2020a; MathWorks, Natick, MA).

3 Results

3.1 Statistical regression models

With the inclusion of tragion-to-top distance, the statistical models for predicting brain length (l_b; in cm), width (w_b; in cm), and volume (v_b; in cm^3) were given by the following equations (all coefficients were statistically significant with $p < 0.05$):

$$l_b = 0.81 \times \text{len}_{\text{hd}} - 0.15 \times \text{circ}_{\text{hd}} - 0.03 \times \text{age} + 0.19 \times \text{trag}_{\text{hd}} + 7.59 \tag{4}$$

$$w_b = 0.66 \times \text{breadth}_{\text{hd}} + 0.10 \times \text{trag}_{\text{hd}} - 0.07 \times \text{len}_{hd} + 3.86 \tag{5}$$

$$v_b = 58.10 \times \text{len}_{\text{hd}} + 53.77 \times \text{breadth}_{\text{hd}} + 84.24 \times \text{trag}_{\text{hd}} - 8.91 \times \text{age} - 1317.6 \tag{6}$$

where len_{hd}, $breadth_{hd}$, $circ_{hd}$ and $trag_{hd}$ are the length, breadth, circumference of the head and tragion-to-top distance (all in cm); age and sex refer to age (in years) and sex

(categorical variable, with 0 for male and 1 for female) information for the given subject. Notably, sex was not selected as a contributing feature in the above regression models.

Excluding tragion-to-top distance, the following regression models were derived (similarly, all coefficients were statistically significant with $p < 0.05$):

$$l_b = 0.82 \times \text{len}_{\text{hd}} - 0.11 \times \text{circ}_{\text{hd}} - 0.03 \times \text{age} + 8.19 \quad (7)$$

$$w_b = 0.67 \times \text{breadth}_{\text{hd}} + 3.77 \quad (8)$$

$$v_b = 40.06 \times \text{circ}_{\text{hd}} - 61.97 \times \text{sex} - 8.83 \times \text{age} - 439.7 \quad (9)$$

Finally, the regression models using age and sex only were the following:

$$l_b = 18.24 - 0.02 \times \text{age} - 0.65 \times \text{sex} \quad (10)$$

$$w_b = 14.07 - 0.01 \times \text{age} - 0.43 \times \text{sex} \quad (11)$$

$$v_b = 1799.10 - 4.63 \times \text{age} - 178.46 \times \text{sex} \quad (12)$$

3.2 Regression model geometrical accuracy

For all brain measurement regressions, performances significantly improved when external head dimensions were included in the statistical models over those only considering age and sex (Table 2). The performances improved slightly when the additional head tragion-to-top measurement was incorporated, compared to those without.

In terms of absolute percentage error (APE) relative to the actual measurements, the two regression models that incorporated head dimensions were statistically indistinguishable ($p > 0.05$), regardless of whether tragion-to-top was utilized. However, they significantly improved over those only considering age and sex, or the generic model that did not incorporate any subject-specific information at all (Fig. 5).

The performance differences were more evident when comparing the number of subjects with brain dimension prediction errors exceeding a given threshold (Fig. 6). At the 5% and 10% threshold levels, the two best performing regression models led to few subjects exceeding the error thresholds, especially for brain length and width. In contrast, the regression model with only age and sex as well as the generic model performed poorly for all brain measures. For example, about 55% the subjects had an APE greater than 5% for brain volume with the generic model, which decreased to 23% of subjects at the 10% threshold.

Table 2 Comparison of adjusted R^2 for regression models with and without tragion-to-top measurement as features, along with that only considering age and sex for predicting brain length, width, and volume (bold indicates best performances)

Adjusted R^2	With tragion-to-top	Without tragion-to-top	Age and sex only
brain length (l_b)	**0.713**	0.693	0.222
brain width (w_b)	**0.620**	0.608	0.170
brain volume (v_b)	**0.720**	0.613	0.405

3.3 Scaled models vs. morphed models for brain strain comparison

Four of the 11 selected subjects were used to graphically compare the two scaled models based on whether tragion-to-top was utilized for statistical regression or not. Except for the smallest and the largest brains, the other two scaled models were virtually identical in mesh outer boundaries, which also matched well with the actual axial MRI (Fig. 7). Some differences were seen for the smallest and largest brains. However, the average mesh surface distances between the two scaled models were within 1 voxel resolution of 1.5 mm. The distance slightly increased (< 1.9 mm) when comparing with the corresponding segmented brain surfaces. These findings suggest accurate brain model geometry overall. For the smallest brain, overlays of the different brain models in 3D are shown in the Supplementary for additional comparisons (Fig. S2).

The three sets of scaled models and the generic WHIM were compared against the morphed models in terms of Dice coefficient across the 11 subjects for geometrical accuracy. In addition, they were compared in terms of peak MPS of the whole brain (Table 3). All scaled models improved geometrical accuracy as well as response accuracy relative to the generic model. Again, the scaled model that utilized tragion-to-top distance as an input feature for regression had the best accuracy, but the improvement was marginal relative to that without using this feature.

For regional peak MPS, the three scaled models were not statistically different ($p > 0.1$ for all comparisons) in terms of R^2 and RMSE (Fig. 8). However, they all significantly improved over the generic model. Only the regression slopes of the two scaled models, with and without TT, were not significantly different from 1.0, indicating no over- or under-estimation existed overall. The same scaled models also had significantly smaller variance compared to the age-and-sex-only model and the generic model.

Using the morphed model as the baseline, the best-performing scaled model (with tragion-to-top included in regression) was compared with the age-and-sex-only model as well as the generic model. Scatter plots for regional peak MPS for two subjects with the smallest or largest brain volume are shown (Fig. 9). In both subjects, the scaled model

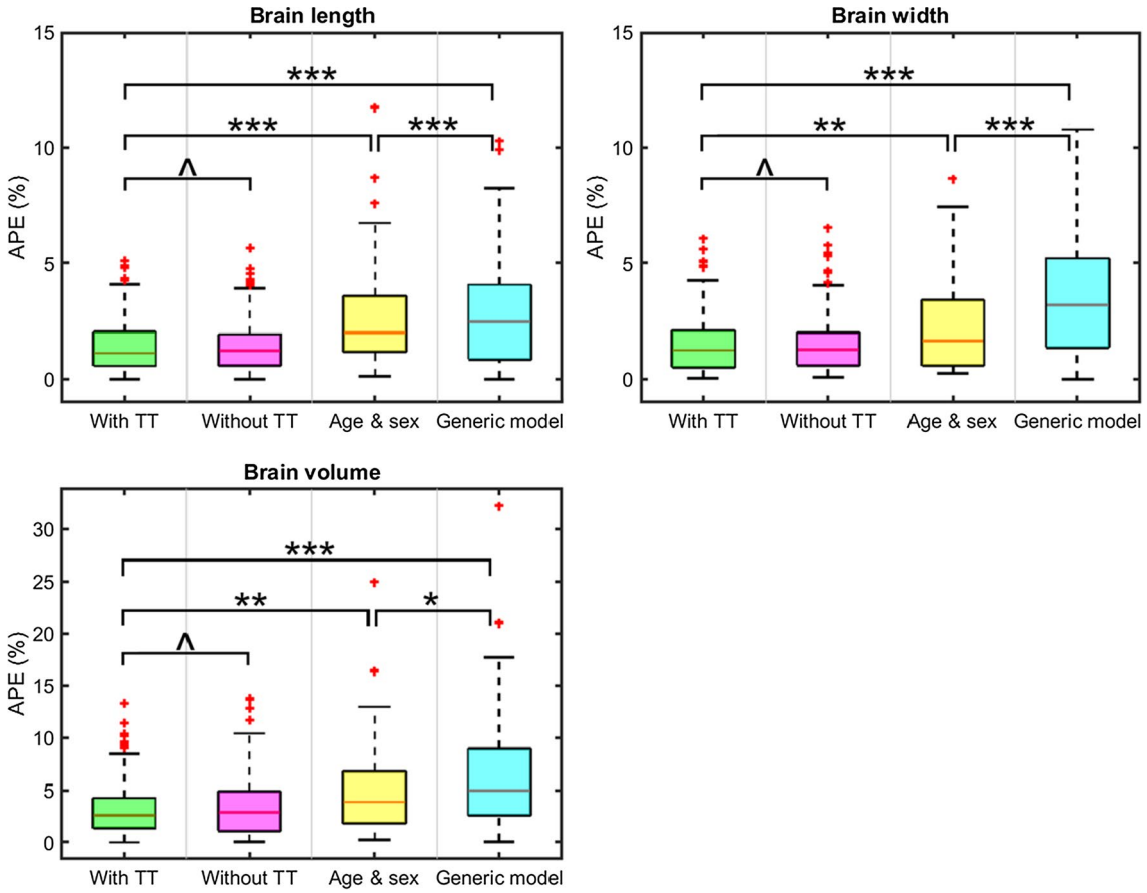

Fig. 5 Boxplot of the absolute percentage errors (APE) between the directly measure brain dimensions (length, width, and volume) for 191 subjects and those predicted using the three statistical models that incorporate head measurements with or without tragion-to-top (TT), and models only relying on age and sex information. Measurements from the generic model are also provided as a reference. Not all statistical relationships are shown to improve clarity. *: $0.0001 < p < 0.05$; **: $1 \times 10^{-6} < p < 0.0001$; ***: $p < 10^{-6}$; ^: $p > 0.05$

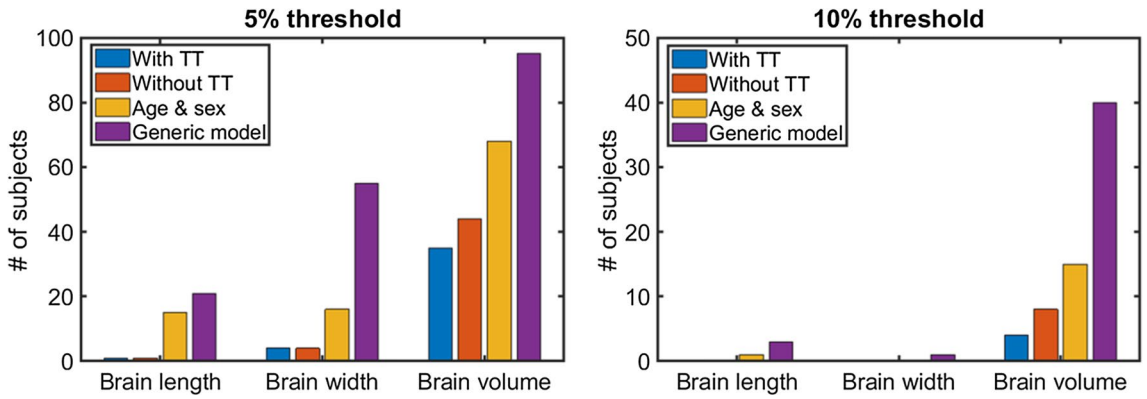

Fig. 6 Summary of the number of subjects with the absolute percentage error (APE) above 5% (**a**) and 10% (**b**) threshold for predicting three brain measurements (brain length, width, and volume) among three sets of regression models (with or without TT, or age-and-sex-only) as well as the generic model

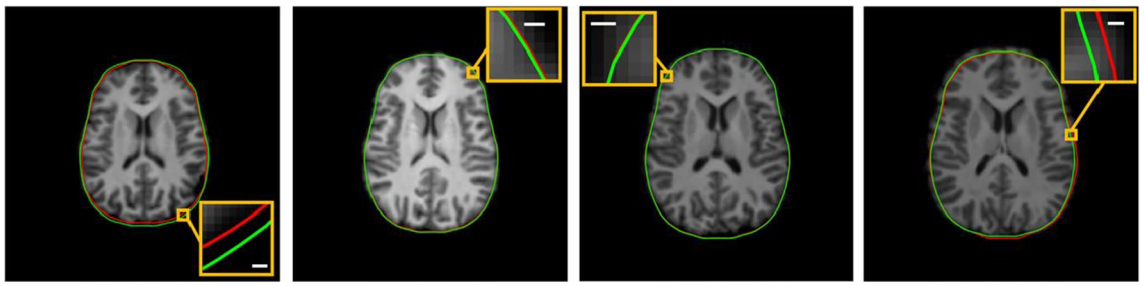

Fig. 7 Comparison of brain mesh outer boundaries overlaid on axial MRI for 4 representative subjects-specific scaled models. From left to right: subject with brain volume the smallest (left: a female subject of age 23) to the largest (right: a male subject of age 20). Red and green lines represent the mesh outer boundaries using the regression model that either incorporated tragion-to-top, or not. For the two subjects in the middle (a female and a male subject both of age 19), their mesh outer boundaries from the two scaled models are virtually identical that also approximate the corresponding axial MRI well. Scale bar length: 2 mm

Table 3 Summary of Dice coefficient of the three scaled models and the generic model relative to the corresponding baseline morphed models for the 11 subjects, along with R^2 and RMSE (including its range) in terms of their peak MPS of the whole brain. The three scaled models are generated using the corresponding set of statistical regression models: with and without tragion-to-top (TT), and age-and-sex-only

	With TT	Without TT	Age and sex	Generic WHIM
Dice coefficient mean ± std (min, max)	**0.977 ± 0.017** (0.942, 0.998)	0.969 ± 0.021 (0.916, 0.988)	0.924 ± 0.042 (0.806, 0.951)	0.901 ± 0.039 (0.803, 0.950)
R^2	**0.908**	0.815	0.686	0.500
RMSE (min, max)	**0.009** (0.001, 0.015)	0.011 (0.001, 0.020)	0.015 (0.002, 0.036)	0.021 (0.001, 0.049)

with tragion-to-top had the highest R^2, smallest RMSE, and with k values closest to 1.0. The generic model performed the worst in all categories.

Finally, the subject with the smallest brain was used to highlight MPS similarities and differences relative to those from the morphed model on two representative axial MRI imaging planes. The two scaled models that included head external features were almost identical (95% of the brain volume had a difference less than 0.01). Therefore, only the one with the inclusion of tragion-to-top in the regression model was illustrated. It had a similar MPS response relative to the morphed counterpart (e.g., 95% of the volume had a difference < 0.02). However, much larger differences were observed for the age-and-sex-only model (e.g., 38% of the brain volume had a difference > 0.02, and 6% volume had a difference > 0.04) and the generic model (e.g., 58% of the brain volume had a difference > 0.02, and 17% volume had a difference > 0.04).

4 Discussion

In this study, we developed a technique to approximate subject-specific brain injury models by linearly scaling a generic counterpart. The three scaling factors along the anatomical axes are based on predictions from statistical regression models established from easily measurable external head dimensions and subject's age and sex information. A notable advantage of our work relative to other statistical models (Danelson et al. 2008) or neuroimage-based techniques (Ji et al. 2015; Miller et al. 2016; Giudice et al. 2020; Li et al. 2020; Alshareef et al. 2021; Li 2021) is that it does not require neuroimages to approximate subject-specific brain models. Our scaled models are comparable to the morphed counterparts in regional brain strains (Fig. 9) as well as detailed whole-brain strains (Fig. 10), but they are much more efficient to generate than mesh warping (< 1 s vs. hours, e.g., Giudice et al. 2020; Li et al. 2020; Li 2021)). Simple linear scaling also maintains virtually the same mesh quality relative to the generic model, as the scaling factors are typically around 0.9–1.1 for most subjects. In contrast, morphed models could degrade mesh quality in regions due to large local displacements from nonrigid registration (confirmed but results not shown).

These notable and appealing advantages of our technique could substantially enhance subject-specificity for future brain impact modeling. The simple linear scaling factors are also ideal for serving as additional inputs to deep learning brain models (Ghazi et al. 2021; Wu et al. 2022) to improve

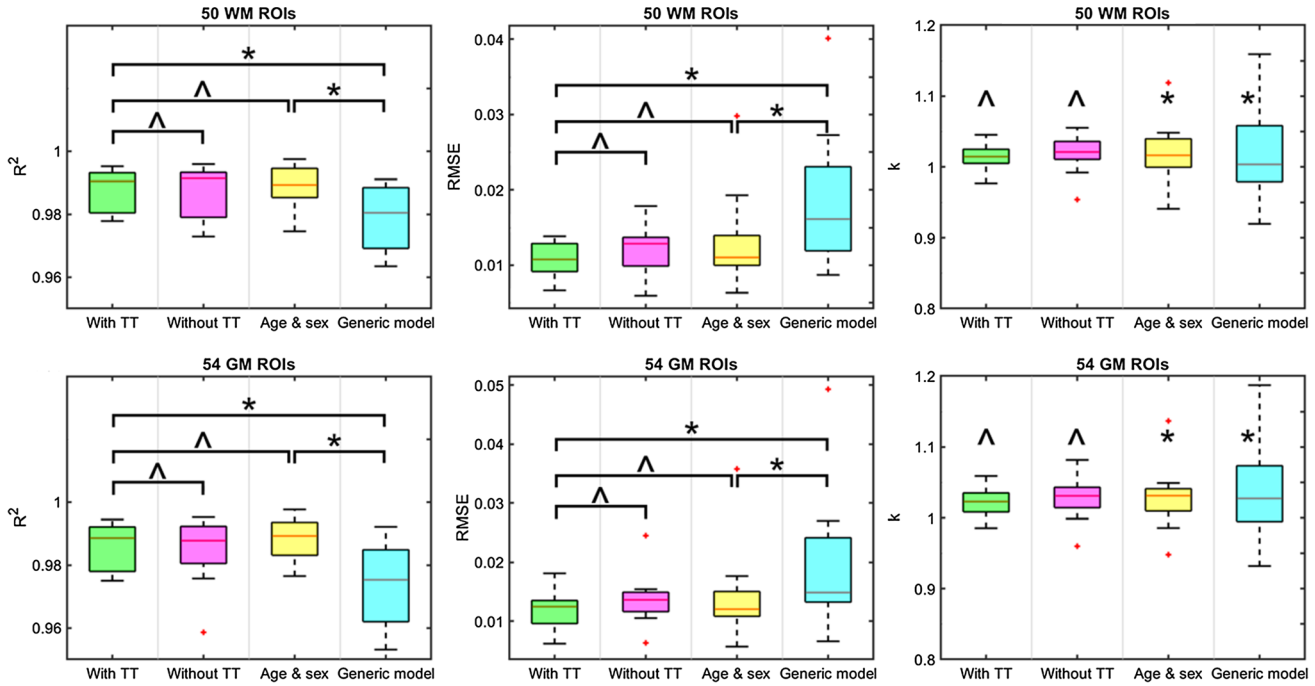

Fig. 8 Boxplot of the R^2, RMSE, and k values for the three scaled models and the generic one using responses from the morphed model as the baseline for the 50 WM ROIs (top) and 54 GM ROIs (bottom). Not all statistical relationships for pairwise comparisons are shown to improve clarity. For k values, statistical tests were conducted to test whether the mean was significantly different from 1.0. *: $p<0.05$; ^: $p>0.05$

subject specificity while instantly estimating detailed brain strains. It is envisioned that such enhanced deep learning models accounting for individual head/brain morphological variations could elevate state-of-the-art and large-scale, population-based brain impact modeling to the next level (Ji et al. 2022).

4.1 Comparison with previous work

By including easily measurable external head dimensions, in addition to age and sex alone (Danelson et al. 2008) as input features, our regression models were significantly more accurate in geometry for all brain measures including length, width, and volume. For example, the adjusted R^2 for the age-and-sex-only model for brain length and width was only in the range of 0.1–0.2, vs. 0.6–0.7 when using additional head dimensions (Table 2). The higher performance of the two best performing scaled models that incorporated head dimensions was also evident when conducting pairwise comparisons in terms of absolute percentage error (Fig. 5) and counting how many subjects had an absolute percentage error greater than the 5% or 10% threshold (Fig. 6). The two best performing scaled models only had a few "failed" cases. In contrast, the scaled model using age and sex information alone and the generic model had many failed cases, especially for brain volume.

Inclusion of the tragion-to-top distance into the regression model also improved the fitting performance over those without (e.g., adjusted R^2 of 0.720 vs. 0.613 for brain volume; Table 2). The stepwise regression consistently identified tragion-to-top as a statistically significant feature for all regression models (Eqns. (4), (5) (6). This was in agreement with the finding that tragion-to-top is a principal component influencing head geometrical variation (Liu et al. 2022). However, the two regression models were statistically indistinguishable when applied to predict brain dimensions in terms of absolute percentage error relative to the actual measurements ($p>0.05$; Fig. 5).

In terms of impact-induced brain strains for the selected 11 subjects, once again, the scaled models that incorporated external head dimensions as features for regression performed the best in terms of R^2 and RMSE for peak MPS of the whole brain (Table 3). In terms of regional peak MPS, the three scaled models all significantly improved over the generic model. However, they were not statistically different among themselves in terms of R^2 and RMSE (Fig. 8). Nevertheless, the regression slope for both the age-and-sex-only model and the generic model was significantly different from 1.0, indicating the two models could under- or overestimate regional strains overall. For example, both considerably overestimated regional peak MPS for the smallest brain, while underestimated for the

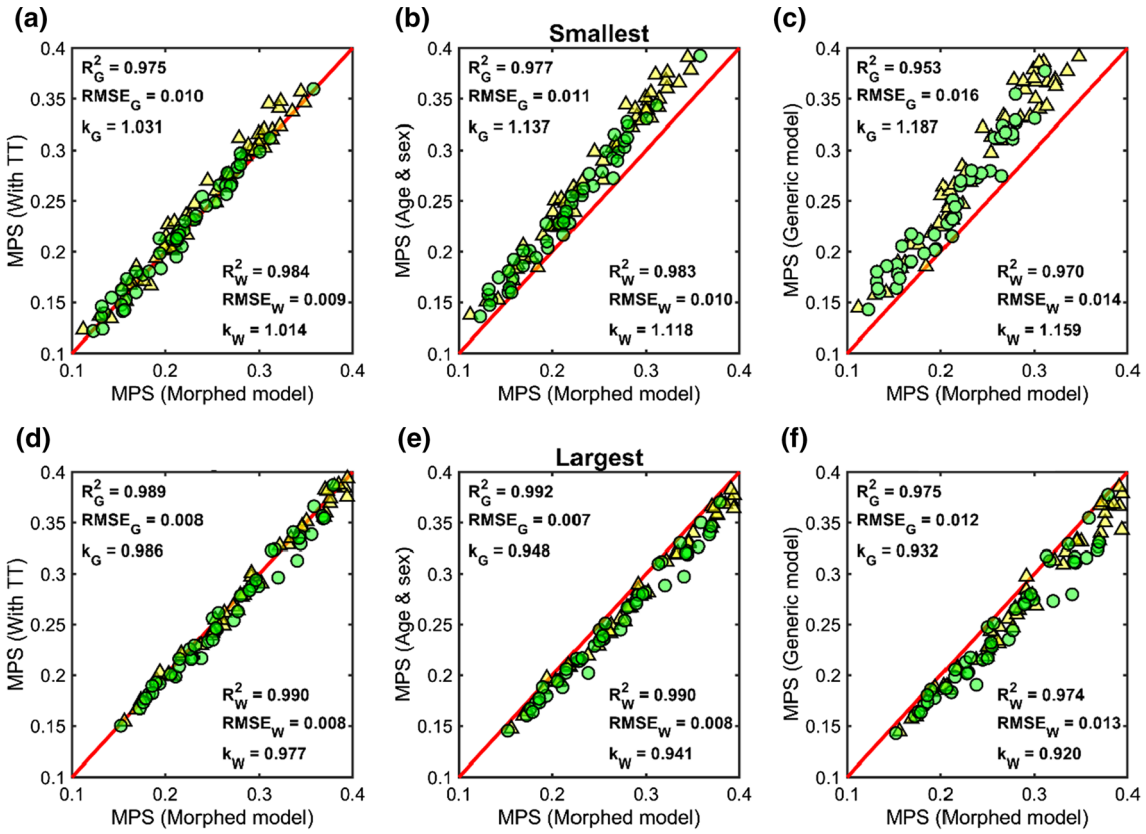

Fig. 9 Scatter plots comparing regional peak MPS in the deep 50 WM and 54 GM ROIs obtained from the best performing scaled models (utilizing tragion-to-top in regression), age-and-sex-only model, and the generic model relative to those from the morphed models for two subjects with the smallest (top) or largest (bottom) brain volume. The R^2, RMSE, and linear regression slope, k, for the two groups of regions are also reported (subscripts "G" and "W" indicate gray matter and white matter ROIs, respectively). Significant over- (top) or underestimation (bottom) occurred for the two subjects using the age-and-sex-only model or the generic model

largest brains (Fig. 9). In contrast, the scaled models based on head external measures had a regression slope not statistically different from 1.0, indicating no overall under- or overestimation in regional peak strains existed. For the same two subjects, their slopes differed from 1.0 by no more than 2–3%.

These findings highlight the necessity of incorporating individual brain morphological variations in head impact simulation. Nevertheless, no statistical difference existed between the two scaled models either using or not using tragion-to-top in terms of both geometrical accuracy and brain strain. This suggested that incorporating tragion-to-top measurement into the regression model may have limited effect on the accuracy in approximating subject-specific models, even though it was identified as a top feature to explain head and brain size variance (Liu et al. 2022). In practice, measuring head length, breadth, and circumference would seem sufficient to generate scaled subject-specific brain models.

Given that external head dimensions can be easily measured on the field (Park et al. 2021) and that individualized neuroimages are not typically available, this study has important implications as it enables large-scale, subject-specific brain injury studies without relying on individual neuroimages in the future. In addition to peak MPS of the whole brain commonly used at present (Li et al. 2020; Fahlstedt et al. 2021; Liu et al. 2021, 2022), we also systematically compared regional peak strains in gray and white matter ROIs. This is an important advancement given the emerging recognition of the importance of strain spatial distribution in studying the biomechanical basis of concussion (Wu et al. 2020; Anderson et al. 2020).

4.2 Subject age and sex

While age was selected in most of the regression models (except for Eqns. (5) and (8) and the corresponding coefficients were all statistically significant, the regression coefficients were relatively small in magnitude, and all were negative. This indicated an overall trend of decreasing brain length/width and volume over age for the population studied (age 14–25). This was consistent with previous findings that

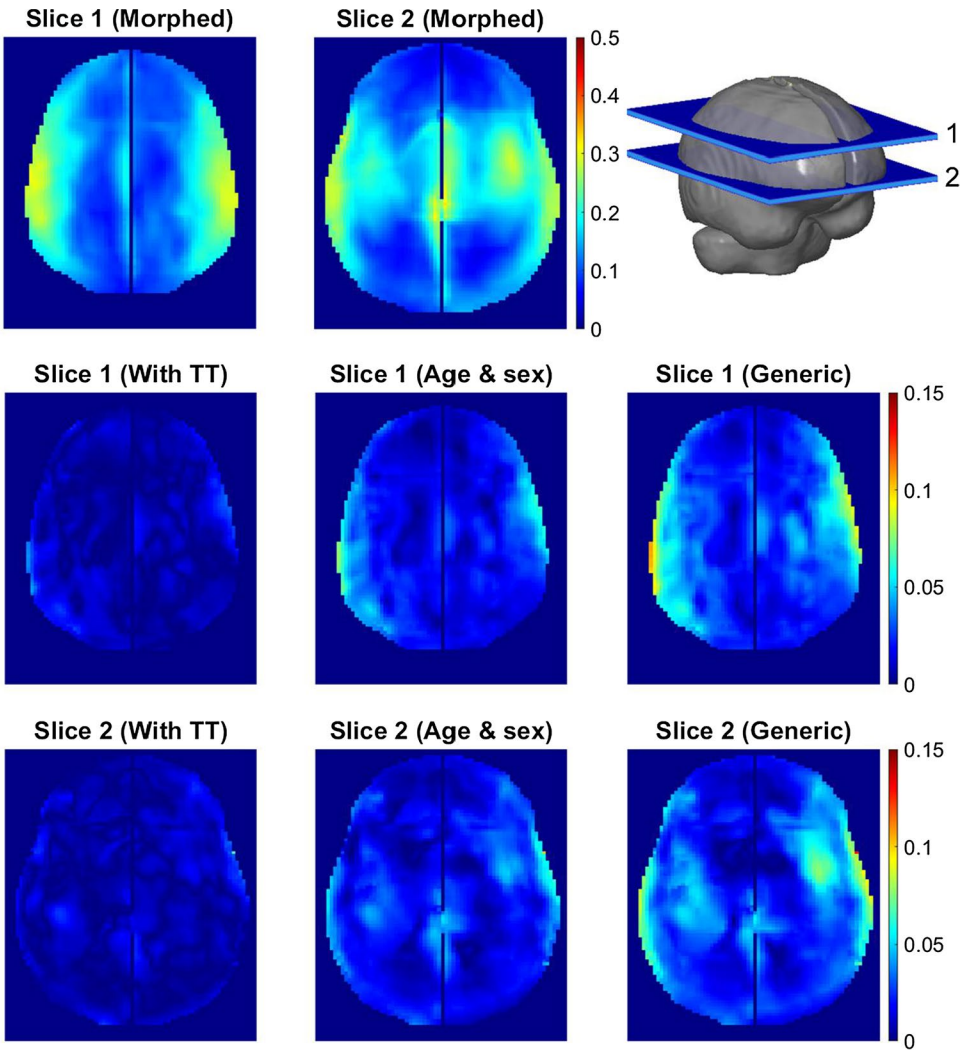

Fig. 10 Resampled peak MPS over the entire impact simulation on two axial planes using the morphed model (top), along with the absolute differences in peak MPS using the best-performing scaled model (with TT), the age-and-sex-only model (Age & sex), and the generic model for the subject with the smallest brain volume

identified brain volume decreasing from adolescence onward but not head circumference (Courchesne et al. 2000; Bartholomeusz et al. 2002). In addition, age was found to correlate with brain length and volume ($p < 0.05$), but not with other head or brain measures ($p > 0.05$). These correlation statistics were consistent with the regression models that incorporated external head dimensions as features.

It is interesting to note that sex was rarely selected as an independent contributing feature in the two sets of regression models that accounted for external head dimensions (except for Eq. (9). However, this does not necessarily indicate that sex was not important. Rather, its effects have already been considered by using other head dimension measures as contributing features. In fact, sex was found to be highly correlated ($p < 0.001$) with all external head measures as well as internal brain measures. When stepwise regression was used, the external measures selection identified external head measures, but not sex, to achieve the best fit.

Because external head dimensions were more effective than age and sex alone in regression, it was not surprising that the quality of the fitting was much improved over the ones that only considered age and sex Eqns. (10), (11), (12); Table 2. The coefficients for both sex and age were negative, indicating that females are generally of smaller brain dimensions, and that the brain shrinks in all dimensions over age for the population studied (age 14–25). The adjusted R^2 values for brain length and width (0.170–0.222) were considerably smaller than that for brain volume (0.405; Table 2), indicating more variations in brain shape for this age group than for brain volume. Finally, for brain length and width, they were mostly dependent on the length and breadth of the head. Even if other features were included, their coefficients were much smaller (Eqns. (4) and (5), Eqns. (7) and (8), which was somewhat expected. Nevertheless, the additional features slightly improved model fitting performance (e.g., adjusted R^2 increased from 0.66 for brain length using head length only, to 0.713; from 0.608 for brain width using head breadth only, to 0.620, when tragion-to-top was included).

4.3 Statistical models to account for morphological variations

Statistical models are commonly used to account for morphological variations (Hu 2018) in developing FE models, such as the rib cage (Wang et al. 2016), liver (Lu and Untaroiu 2014), brain (Danelson et al. 2008), and skull (Urban et al. 2016). They can be broadly classified into three categories, using either multivariate regression models, generalized Procrustes alignment (GPA), or principal component analysis (PCA). Multivariate regression models correlate morphological parameters of the anatomy along with age, sex, and stature for geometry prediction (Bartholomeusz et al. 2002; Wang et al. 2004, 2016). GPA-based method is applied to match geometrical landmarks and meshes of the FE models from subjects for further statistical analysis, which is widely used in anthropology and anatomy (Dijksterhuis and Gower 1991; Slice 2005). In comparison, PCA-based method relies on the principal component (PC) scores to characterize shape variation. This method could also be used as preprocessing to correlate with other features (e.g., age, sex, and body mass) for subject-specific anatomical geometry estimation (Shi et al. 2014).

Nevertheless, these models operate on the anatomy of interest directly. In comparison, our regression-based method approximates brain morphology *indirectly* using features from external head, without relying on neuroimages or landmark identifications that may be time consuming and sensitive to noises (Wu et al. 2019a). This contributes to the general statistical methods for approximating subject-specific models.

4.4 Limitations and further development

Due to the relatively limited age range (14–25 years), the regression models may not be extended to younger subjects (e.g., <7 year old), where greater variability is expected and that the head and brain dimensions have a different growth trend (e.g., rapid growth of brain volume and head circumference vs. shrinking brain size with more or less constant head circumference for the older subjects (Courchesne et al. 2000; Bartholomeusz et al. 2002)). In addition, the sample size for females ($N=50$) was also smaller than that of the males ($N=141$). Therefore, there may be more accuracy degradation for female subjects. Nevertheless, the techniques developed in this study can be readily applied to the appropriate neuroimaging dataset, which can be explored in the future. This may be important for model-based investigations of TBI for younger and female athletes.

We did not use the CT data in (Liu et al. 2022) to augment our MRI data for analysis, because they do not capture the same anatomical surfaces (skull inner surface vs. brain outer surface and skull outer surface vs. scalp outer surface). Nevertheless, some additional analysis was performed to probe the sensitivity of the regression model coefficients relative to the number of subjects. By randomly halving the subject numbers, most coefficients differed by less than 5%, with a few differed by 11–15% (Tables S1–S3 in the Supplementary). These results suggest reasonably stable results in our study.

Another limitation is that variations of internal brain anatomies such as ventricles are not considered in this study. Neuroimage-based mesh warping may have the benefit of accounting for these internal brain anatomies (Giudice et al. 2020; Li et al. 2020; Li 2021); albeit, at the expense of necessitating neuroimages in the first place. It is also possible to further extend our work to internal anatomies (Danelson et al. 2008). However, there are a few considerations worthy of note before such an effort. First, to appropriately model internal brain anatomies, their material properties as well as internal boundary conditions such as those between the sulci folding are also necessary. However, they are not well characterized at present. In addition, current experimental data for model validation are not sufficient to distinguish or to confirm model biofidelity for strain responses (Zhao and Ji 2020; Zhao et al. 2021). Therefore, although models with detailed internal anatomical representations may offer improved strain distributions, additional verification from pathological neuroimages is necessary to confirm their effectiveness. From the model utility perspective, detailed brain strains are not yet commonly used for any result interpretation (Fahlstedt et al. 2021; Ji et al. 2022). Given these considerations, therefore, simple linear scaling may be sufficient for certain applications to approximate subject-specific models due to the ease of use and efficiency, and no need for neuroimages.

Finally, brain strain evaluations were only conducted using one representative head impact and one specific head injury model. More comprehensive evaluations using impact kinematics over a range of impact directions and severities are necessary to better understand the role of brain morphological variation on strain. In addition, comparison in terms of white matter fiber strain (Giordano and Kleiven 2014; Ji et al. 2015; Sahoo et al. 2016) is also warranted, given its improved characterization of tissue strains. However, this is beyond the scope of the current study and will be pursued in the future. Lastly, evaluation with other head injury models may also help confirm findings in this study, for which the techniques developed herein would remain equally valid. The evaluations can be achieved by replacing the head and brain dimensions of the generic model accordingly (Table 1).

Supplementary Information The online version contains supplementary material available at https://doi.org/10.1007/s10237-022-01638-6.

Acknowledgements National Institute of Neurological Disorders and Stroke, R01 NS092853, Songbai Ji, Division of Civil, Mechanical and Manufacturing Innovation, 2114697, Songbai Ji

References

Alshareef A, Giudice JS, Forman J et al (2018) A novel method for quantifying human in situ whole brain deformation under rotational loading using sonomicrometry. J Neurotrauma 35:780–789. https://doi.org/10.1089/neu.2017.5362

Alshareef A, Wu T, Giudice JS, Panzer MB (2021) Toward subject-specific evaluation: methods of evaluating finite element brain models using experimental high-rate rotational brain motion. Biomech Model Mechanobiol. https://doi.org/10.1007/s10237-021-01508-7

Anderson ED, Giudice JS, Wu T et al (2020) Predicting concussion outcome by integrating finite element modeling and network analysis. Front Bioeng Biotechnol 8:309. https://doi.org/10.3389/fbioe.2020.00309

Atsumi N, Nakahira Y, Tanaka E, Iwamoto M (2018) Human brain modeling with its anatomical structure and realistic material properties for brain injury prediction. Ann Biomed Eng 46:736–748. https://doi.org/10.1007/s10439-018-1988-8

Bartholomeusz HH, Courchesne E, Karns CM (2002) Relationship between head circumference and brain volume in healthy normal toddlers, children, and adults. Neuropediatrics 33:239–241. https://doi.org/10.1055/s-2002-36735

Bian K, Mao H (2020) Mechanisms and variances of rotation-induced brain injury: a parametric investigation between head kinematics and brain strain. Biomech Model Mechanobiol 1–19:2323–2341. https://doi.org/10.1007/s10237-020-01341-4

Bradshaw D, Morfey C (2001) Pressure and shear response in brain injury models. In: Proceedings of the 17th International Technical Conference on the Enhanced Safety of Vehicles. Amsterdam, The Netherlands, pp 1–10

Centers for Disease Control and Prevention (2007) Nonfatal traumatic braininjuries from sports and recreation activities–United States, 2001–2005. In: MMWRMorb Mortal Wkly Rep. pp 56(29): 733–737

Chan D, Knutsen AK, Lu Y-C et al (2018) Statistical characterization of human brain deformation during mild angular acceleration measured in vivo by tagged MRI. J Biomech Eng 140:1–13. https://doi.org/10.1115/1.4040230

Chen Y, Ostoja-Starzewski M (2010) MRI-based finite element modeling of head trauma: spherically focusing shear waves. Acta Mech 213:155–167. https://doi.org/10.1007/s00707-009-0274-0

Collins CL, Fletcher EN, Fields SK et al (2014) Neck strength: a protective factor reducing risk for concussion in high school sports. J Prim Prev 35:309–319. https://doi.org/10.1007/S10935-014-0355-2/TABLES/6

Courchesne E, Chisum HJ, Townsend J et al (2000) Normal brain development and aging quantitative analysis at in vivo mr imaging in healthy volunteers. Radiology 216:672–682

Danelson KA, Geer CP, Stitzel JD et al (2008) Age and gender based biomechanical shape and size analysis of the pediatric brain. Stapp Car Crash J 52:59–81

Dewan MC, Rattani A, Gupta S et al (2019) Estimating the global incidence of traumatic brain injury. J Neurosurg 130:1080–1097. https://doi.org/10.3171/2017.10.JNS17352

Dijksterhuis GB, Gower JC (1991) The interpretation of generalized procrustes analysis and allied methods. Food Qual Prefer 3:67–87. https://doi.org/10.1016/0950-3293(91)90027-C

Draper NR, Smith H (1998) Applied Regression Analysis. Wiley

Fahlstedt M, Abayazid F, Panzer MB et al (2021) Ranking and rating bicycle helmet safety performance in oblique impacts using eight different brain injury models. Ann Biomed Eng 49:1097–1109. https://doi.org/10.1007/s10439-020-02703-w

Ferdinand Pennock K, McKenzie B, McClemont Steacy L, Mainwaring L (2020) Under-reporting of sport-related concussions by adolescent athletes: a systematic review. Int Rev Sport Exerc Psychol pp 1–27

Garimella HT, Menghani RR, Gerber JI et al (2019) Embedded finite elements for modeling axonal injury. Ann Biomed Eng 47:1–19. https://doi.org/10.1007/s10439-018-02166-0

Ghajari M, Hellyer PJ, Sharp DJ (2017) Computational modelling of traumatic brain injury predicts the location of chronic traumatic encephalopathy pathology. Brain 140:333–343. https://doi.org/10.1093/brain/aww317

Ghazi K, Wu S, Zhao W, Ji S (2021) Instantaneous whole-brain strain estimation in dynamic head impact. J Neurotrauma 38:1023–1035. https://doi.org/10.1089/neu.2020.7281

Giordano C, Kleiven S (2014) Evaluation of axonal strain as a predictor for mild traumatic brain injuries using finite element modeling. Stapp Car Crash J 58:29–61. https://doi.org/10.4271/2014-22-0002

Giordano C, Zappalà S, Kleiven S (2017) Anisotropic finite element models for brain injury prediction: the sensitivity of axonal strain to white matter tract inter-subject variability. Biomech Model Mechanobiol 16:1269–1293. https://doi.org/10.1007/s10237-017-0887-5

Giudice JS, Alshareef A, Wu T et al (2020) An image registration-based morphing technique for generating subject-specific brain finite element models. Ann Biomed Eng. https://doi.org/10.1007/s10439-020-02584-z

Hardy WN, Mason MJ, Foster CD et al (2007) A study of the response of the human cadaver head to impact. Stapp Car Crash J 51:17–80. https://doi.org/10.4271/2019-22-0001

Hu J (2018) Parametric human modelling. Basic finite element method as applied to injury biomechanics. Elsevier, pp 417–445. https://doi.org/10.1016/B978-0-12-809831-8.00010-6

Iverson GL, Gardner AJ, Terry DP et al (2017) Predictors of clinical recovery from concussion: a systematic review. Br J Sports Med 51:941–948. https://doi.org/10.1136/bjsports-2017-097729

Ji S, Ford JCJC, Greenwald RM et al (2011) Automated subject-specific, hexahedral mesh generation via image registration. Finite Elem Anal Des 47:1178–1185. https://doi.org/10.1016/j.finel.2011.05.007

Ji S, Zhao W, Ford JC et al (2015) Group-wise evaluation and comparison of white matter fiber strain and maximum principal strain in sports-related concussion. J Neurotrauma 32:441–454. https://doi.org/10.1089/neu.2013.3268

Ji S, Ghajari M, Mao H et al (2022) Use of brain biomechanical models for monitoring impact exposure in contact sports. Ann Biomed Eng. https://doi.org/10.1007/s10439-022-02999-w

Kleiven S, von Holst H (2002) Consequences of head size following trauma to the human head. J Biomech 35:153–160. https://doi.org/10.1016/S0021-9290(01)00202-0

Knutsen AK, Magrath E, McEntee JE et al (2014) Improved measurement of brain deformation during mild head acceleration using a novel tagged MRI sequence. J Biomech 47:3475–3481. https://doi.org/10.1016/j.jbiomech.2014.09.010

Laker SR (2011) Epidemiology of concussion and mild traumatic brain injury. PM&R 3:S354–S358. https://doi.org/10.1016/j.pmrj.2011.07.017

Langlois JA, Rutland-Brown W, Wald MM (2006) The epidemiology and impact of traumatic brain injury a brief overview. J Head Trauma Rehabil 21:375–378

Lee J-H, Shin S-J, Istook C (2006) Analysis of human head shapes in the United States. Int J Hum Ecol 7:77–83

Li X (2021) Subject-specific head model generation by mesh morphing: a personalization framework and its applications. Front Bioeng Biotechnol. https://doi.org/10.3389/fbioe.2021.706566

Li Z, Hu J, Reed MP et al (2011) Development, validation, and application of a parametric pediatric head finite element model for impact simulations. Ann Biomed Eng 39:2984–2997. https://doi.org/10.1007/s10439-011-0409-z

Li Z, Han X, Ge H, Ma C (2016) A semi-automatic method of generating subject-specific pediatric head finite element models for impact dynamic responses to head injury. J Mech Behav Biomed Mater 60:557–567. https://doi.org/10.1016/j.jmbbm.2016.03.021

Li X, Zhou Z, Kleiven S (2020) An anatomically accurate and personalizable head injury model: significance of brain and white matter tract morphological variability on strain. Biomech Model Mechanobiol. https://doi.org/10.1101/2020.05.20.105635

Liu Y, Domel AG, Cecchi NJ et al (2021) Time window of head impact kinematics measurement for calculation of brain strain and strain rate in american football. Ann Biomed Eng. https://doi.org/10.1007/s10439-021-02821-z

Liu JL, Jin J, (Judy), Eckner JT et al (2022) Influence of morphological variation on brain impact responses among youth and young adults. J Biomech 135:111036. https://doi.org/10.1016/J.JBIOMECH.2022.111036

Lu YC, Untaroiu CD (2014) A statistical geometrical description of the human liver for probabilistic occupant models. J Biomech 47:3681–3688.

McAllister TW, Ford JC, Ji S et al (2012) Maximum principal strain and strain rate associated with concussion diagnosis correlates with changes in corpus callosum white matter indices. Ann Biomed Eng 40:127–140. https://doi.org/10.1007/s10439-011-0402-6

Miller LE, Urban JE, Stitzel JD (2016) Development and validation of an atlas-based finite element brain model model. Biomech Model 15:1201–1214. https://doi.org/10.1007/s10237-015-0754-1

Mollayeva T, El-Khechen-Richandi G, Colantonio A (2018) Sex & gender considerations in concussion research. Concussion 3:CNC51. https://doi.org/10.2217/cnc-2017-0015

Park G, Gabler LF, Bailey AM et al (2021) Head shape analysis of National Football League Players. Proc Inst Mech Eng Part P J Sports Eng Technol. https://doi.org/10.1177/17543371211020614

Rivara FP, Astley SJ, Clarren SK et al (1999) Fit of bicycle safety helmets and risk of head injuries in children. Inj Prev 5:194–197. https://doi.org/10.1136/IP.5.3.194

Rollins JD, Collins JS, Holden KR (2010) United States head circumference growth reference charts: birth to 21 years. J Pediatr 156:907-913.e2. https://doi.org/10.1016/j.jpeds.2010.01.009

Rowson B, Duma SM (2020) A review of on-field investigations into the biomechanics of concussion in football and translation to head injury mitigation strategies. Ann Biomed Eng 48:1–17

Sahoo D, Deck C, Willinger R (2016) Brain injury tolerance limit based on computation of axonal strain. Accid Anal Prev 92:53–70. https://doi.org/10.1016/j.aap.2016.03.013

Sanchez EJ, Gabler LF, Good AB et al (2018) A reanalysis of football impact reconstructions for head kinematics and finite element modeling. Clin Biomech 64:82–89. https://doi.org/10.1016/j.clinbiomech.2018.02.019

Shattuck D, Mirza M, Adisetiyo V et al (2008) Construction of a 3D probabilistic atlas of human cortical structures. Neuroimage 39:1064–1080

Shi X, Cao L, Reed MP et al (2014) A statistical human rib cage geometry model accounting for variations by age, sex, stature and body mass index. J Biomech 47:2277–2285. https://doi.org/10.1016/J.JBIOMECH.2014.04.045

Slice DE (2005) Modern morphometrics in physical anthropology. Mod Morphometrics Phys Anthropol. https://doi.org/10.1007/0-387-27614-9

Smith SM (2002) Fast robust automated brain extraction. Hum Brain Mapp 17:143–155. https://doi.org/10.1002/HBM.10062

Takhounts EG, Ridella SA, Tannous RE et al (2008) Investigation of traumatic brain injuries using the next generation of simulated injury monitor (SIMon) finite element head model. Stapp Car Crash J 52:1–31

Tang Y, Hojatkashani C, Dinov ID et al (2010) The construction of a Chinese MRI brain atlas: a morphometric comparison study between Chinese and Caucasian cohorts. Neuroimage 51:33–41. https://doi.org/10.1016/J.NEUROIMAGE.2010.01.111

Thai KT, McIntosh AS, Pang TY (2015) Bicycle helmet size, adjustment, and stability. Traffic Inj Prev 16:268–275. https://doi.org/10.1080/15389588.2014.931948

Urban JE, Weaver AA, Lillie EM et al (2016) Evaluation of morphological changes in the adult skull with age and sex. J Anat 229:838–846. https://doi.org/10.1111/JOA.12247

Varentsova A, Zhang S, Arfanakis K (2014) Development of a high angular resolution diffusion imaging human brain template. Neuroimage. https://doi.org/10.1016/j.neuroimage.2014.01.009

Wang SC, Brede C, Lange D et al (2004) Gender differences in hip anatomy: possible implications for injury tolerance in frontal collisions. Annu Proc Assoc Adv Automot Med 48:287

Wang Y, Cao L, Bai Z et al (2016) A parametric ribcage geometry model accounting for variations among the adult population. J Biomech 49:2791–2798

Wu J, Cai M, Li J et al (2019a) Development and validation of a semi-automatic landmark extraction method for mesh morphing. Med Eng Phys 70:62–71. https://doi.org/10.1016/J.MEDENGPHY.2019.04.007

Wu T, Alshareef A, Giudice JS, Panzer MB (2019b) Explicit modeling of white matter axonal fiber tracts in a finite element brain model. Ann Biomed Eng. https://doi.org/10.1007/s10439-019-02239-8

Wu S, Zhao W, Rowson B et al (2020) A network-based response feature matrix as a brain injury metric. Biomech Model Mechanobiol 19:927–942. https://doi.org/10.1007/s10237-019-01261-y

Wu S, Zhao W, Ji S (2022) Real-time dynamic simulation for highly accurate spatiotemporal brain deformation from impact. Comput Methods Appl Mech Eng 394:114913. https://doi.org/10.1016/J.CMA.2022.114913

Yang KH, Hu J, White NA et al (2006) Development of numerical models for injury biomechanics research: a review of 50 years of publications in the Stapp Car Crash Conference. Stapp Car Crash J 50:429–490. https://doi.org/10.4271/2006-22-0017

Zhao W, Ji S (2019) White matter anisotropy for impact simulation and response sampling in traumatic brain injury. J Neurotrauma 36:250–263. https://doi.org/10.1089/neu.2018.5634

Zhao W, Ji S (2020) Displacement- and strain-based discrimination of head injury models across a wide range of blunt conditions. Ann Biomed Eng 20:1661–1677. https://doi.org/10.1007/s10439-020-02496-y

Zhao W, Ji S (2022) Cerebral vascular strains in dynamic head impact using an upgraded model with brain material property heterogeneity. J Mech Behav Biomed Mater 126:104967. https://doi.org/10.1016/j.jmbbm.2021.104967

Zhao W, Ruan S, Ji S (2015) Brain pressure responses in translational head impact: a dimensional analysis and a further computational study. Biomech Model Mechanobiol 14:753–766. https://doi.org/10.1007/s10237-014-0634-0

Zhao W, Cai Y, Li Z, Ji S (2017) Injury prediction and vulnerability assessment using strain and susceptibility measures of the deep white matter. Biomech Model Mechanobiol 16:1709–1727. https://doi.org/10.1007/s10237-017-0915-5

Zhao W, Wu Z, Ji S (2021) Displacement error propagation from embedded markers to brain strain. J Biomech Eng 143:1–10. https://doi.org/10.1115/1.4051050

Zhou Z, Li X, Kleiven S (2019) Biomechanics of acute subdural hematoma in the elderly: a fluid-structure interaction study. J Neurotrauma 36:2099–2108. https://doi.org/10.1089/neu.2018.6143